Sheet pile groups as an alternative foundation solution to cast in-situ concrete piles

Author 1

- Jignasha P Panchal, MEng, PhD
- Honorary fellow at City, University of London, UK and Civil Engineer at Keltbray Piling, UK
- ORCID number: 0000-0001-9342-239X
-

Author 2

- Andrew M McNamara, MSc, PhD
- Department of Civil Engineering, City, University of London, UK
- ORCID number: 0000-0002-3452-0800

Author 3

- Richard J Goodey, BEng, PhD
- Department of Civil Engineering, City, University of London, UK
- ORCID number: 0000-0002-9166-8393

Abstract

Concrete piles have become a common high load bearing foundation solutions providing end bearing and frictional resistance along the shaft. They are typically used for founding commercial or residential blocks with a design life of approximately 50 years. Following this the superstructure is decommissioned and may be demolished. However, piles are difficult to remove and therefore future developers can incur significant expense and programme delays in preparing the site to avoid obstructions. If removed, concrete piles are required to be broken down which is a slow and laborious process. However, a foundation solution has been developed that allows foundations to be installed and extracted with relative ease whilst still achieving a similar, if not improved capacity. This solution has been defined as a hybrid foundation comprising deep sheet piles for shaft resistance and a pile cap as a shallow foundation. The hybrid pile offers significant advantages over concrete piles include ease of installation, extraction, reuse and economy. Axial capacity of individual sheet piles is low, however geometrically arranging sheet piles; was shown to offer comparable or improved

capacity over conventional concrete piles. The results from a series of centrifuge tests are presented in this paper.

Keywords

Bearing capacity; Centrifuge modelling; Piles & piling; Sheet piles & cofferdams; Urban regeneration

Notations

α	Adhesion factor
Ab	Area of pile base
As	Area of pile shaft
B	Width of shallow foundation
CFA	Continuous flight auger
D	Depth of shallow foundation
g	Acceleration due to gravity
H	Length of piled foundation
ID	Inner diameter
LVDT	Linear variable differential transformer
N_c	Bearing capacity factor as a function of pile diameter and length
OD	Outer diameter
PPT	Pore pressure transducer
Qb	End bearing pile capacity
Qs	Skin friction pile capacity
Qult	Ultimate pile capacity at failure
S_u	Soil undrained shear strength
γ	Bulk unit weight of soil

Background

'Hybrid foundations' comprise elements of both deep and shallow foundations and the term typically relates to deep ground improvement and piled rafts (O'Brien, 2012). Hybrid foundations apply structural loads across the shallow foundation before transferring them along the length of the piles. O'Brien explains that hybrid foundation systems are designed to mobilise a majority of the pile shaft capacity to control settlement, whilst the shallow foundation resists bearing capacity failure.

Hybrid foundations are common for offshore applications, comprising shallow foundations reinforced with vertical plates around the perimeter to resist vertical, horizontal and moment loading. Bransby & Yun (2009) show that skirted foundation capacity is governed by embedment ratios. Furthermore, soil enclosed within the skirt may be considered as solid when the foundation is designed purely for axial loading.

This paper considers an alternative hybrid foundation arrangement, whereby sheet piles are aligned to form a closed pile group and a pile cap, cast within the group, behaves as a shallow foundation. Previous studies have shown that this hybrid foundation is a feasible foundation solution capable of achieving similar or improved bearing capacity to conventional solid piles (Panchal *et al*., 2016; 2018a; 2018b).

The shape of the sheet pile groups were varied in this study, the steel piles were also perforated and the B/D ratio was investigated. The initial series of tests comprised a sheet pile group and a solid circular shafted model pile; representative of driven or cast in-situ piles. Consistency between the solid conventional pile test results was obtained, lending confidence to the modelling technique. Consequently the latter part of the experimental series compared a range of sheet pile combinations.

All piles were tested in overconsolidated clay samples and two piles were loaded simultaneously. The results showed that the hybrid pile provided a more effective foundation solution compared with the smooth shafted solid circular pile. The capacity of a sheet pile

group foundation was shown to be further improved by perforating the shaft, varying the geometry from a circle to a square and increasing the shaft area as opposed to increasing the area of the pile base.

Aims and objectives:

To date, a total of seven centrifuge tests at 50*g* have been conducted and this paper aims to draw together the results from these centrifuge tests. Back analysis of the test results was conducted to establish the influence of a number of parameters on the adhesion factor (α). A brief summary of each test will be provided and the validity of the results will be discussed in this paper.

Soil model

Centrifuge tests were conducted in a 420mm diameter stainless steel tub, 300mm deep, in which Speswhite kaolin clay was consolidated. It was necessary to produce a deep soil sample which was achieved by bolting a 300mm deep extension to the top of the centrifuge tub. The internal walls of the tub and extension were lubricated with a thin layer of waterpump grease in order to limit the friction between the clay and tub. Sheets of porous plastic and filter paper were placed at the bottom of the tub before the slurry was poured. Clay slurry mixed in an industrial ribbon mixer to a water content of 120%, twice the liquid limit of Speswhite kaolin, comprised powdered Speswhite kaolin clay powder and distilled water. Speswhite kaolin was used for this particular series of experiments owing to its well established properties and grain size and consequently, its high permeability; which makes Speswhite kaolin a suitable clay for centrifuge modelling.

The slurry was carefully placed in the centrifuge tub to a height of 550mm using a scoop and palette knife. The slurry was agitated frequently to prevent air entrapment in the sample.

Upon reaching the final slurry height, the sample was sandwiched between another sheet of porous plastic and filter paper. The centrifuge tub was transferred to a hydraulic press where pipes were connected to drainage taps in the base of the centrifuge tub and a tightly fitting platen was lowered onto the sample. Herringbone channels at the base of the centrifuge tub lead to the drainage taps and permit consolidation. Holes in the top platen also allowed drainage from the top of the sample, halving the drainage path length and therefore increasing the rate of consolidation.

The effective stress acting on the sample was gradually increased to 500kPa and the day prior to testing, the sample was swelled back to 250kPa. This produced an overconsolidated sample that was reasonably stiff and enabled clean and accurate model making.

Apparatus

The experiments were conducted at the London Geotechnical Centrifuge Centre at City, University of London. They were tested on the Accutronic 661 beam centrifuge which has an effective radius of 1.8m.

This project relied on a bespoke loading frame that could accommodate load cells, LVDTs and an actuated loading beam all acting concurrently to establish the load-settlement curves for the various foundations. The loading frame designed by Gorasia (2013) was used for this series of tests as it had been previously designed for a similar function and could be seated on a circular tub, as illustrated in FIGURE 1. Affixed to the frame was a 5kN actuator that was secured to a stiff loading beam to which two miniature 5kN load cells could be screwed into the loading beam at 210mm centres. Two pairs of LVDT clamps were attached to brackets extending from the loading beam from which average settlements could be computed and checks made to determine whether the piles were loaded eccentrically.

Two pile types were modelled; solid circular piles, representative of a cast in-situ or driven pile, and sheet pile groups, that were arranged in various geometries and sizes. The

maximum pile size was 60mm in diameter and 180mm long, modelling a 3m diameter and 9m long pile at prototype scale. The solid circular piles, illustrated in FIGURE 2A, were subdivided into rough and smooth model piles. The rough solid piles comprised an aluminium 48mmOD closed ended tubular core and a 6mm thick resin layer cast around it in-situ. Plastic dowel bars, 60mm in length, were slotted through the tube perpendicular to the shaft which acted as spacers for the tube and ensured that the core of the pile remained vertical and that an even layer of resin was cast around the pile. A 10mm thick Perspex disc 20mm in diameter was glued to the base of the tube and ensured resin was also cast to the base of the pile. Similarly, the smooth solid pile was formed from a 60mmOD aluminium closed ended tube that slotted into a pre-cut bore. Following the initial two centrifuge tests, the void in the centre of the solid pile tubes were ballasted to ensure the weight of the total pile was equal to the weight of soil that had been removed to mitigate the effects of buoyancy.

The sheet piles, formed from 0.5mm thick sheets of stainless steel, were pressed into shape using a bespoke tool that produced a repeated pattern with 6mm deep ribs at 18mm centres. FIGURE 2B illustrates a cross section of the sheet pile group in-situ. The large square and circular sheet pile group foundations were formed into shape from a single sheet and welded at the seam. The small square sheet pile group was produced from four individual ribbed sheets cut to size and spot welded along each edge in order to achieve the required dimensions. FIGURE 3A illustrates photographs of various sheet pile and solid pile elevations of the model piles used in the experiments and TABLE 1 presents the nominal pile dimensions in plan.

Loading caps were designed and machined from aluminium for both solid and sheet piles which provided a platform on which the LVDTs and load cells reacted against. The sheet pile load caps incorporated a model capping beam that laterally restrained the crest of the sheet piles, preventing them from opening when loaded and also ensured the geometry of the pile remained intact.

As the test series progressed, modifications were made to the circular sheet pile in order to establish whether α could be enhanced. This comprised 5mm diameter holes drilled at 30mm centres along the internal shaft ribs.

General model making procedure

A day prior to model making, the sample was swelled to 250kPa and a deaired miniature Druck PDCR81 pore pressure transducer (PPT) was installed at a depth of 150mm below the top of the tub to the centre of the model before being backfilled with slurry mixed to a water content of 120%. It is widely accepted that pore pressure changes around piles during loading are concentrated immediately around the pile. Consequently, the purpose of the PPT installed in the model was simply to monitor the dissipation of excess pore pressures as the model reconsolidated in flight.

The following day, all standing water was removed from the sample and the drainage taps were closed. After raising the platen from the model the extension was removed and a series of wire cutters were used to trim the sample flush with the top of the centrifuge tub, as shown in FIGURE 4A. PlastiDip, an aerosol applied synthetic flexible rubber membrane, was immediately sprayed across the model surface to prevent the sample from drying out excessively, whilst the two test sites remained uncovered.

The models were prepared under 1g conditions; although the modelling process is not a direct representation of the prototype construction event the model assembly processes are comparable between the two piles tested in each soil sample. Following application of PlastiDip the loading frame was aligned above the model and the loading beam was lowered onto the sample until the load cell pins indented the soil surface and established the pile centres. The sheet piles were installed with relative ease as they were aligned central to the indentation, illustrated in FIGURE 4B, and embedded using the hydraulic press platen to a depth of 180mm, as demonstrated in FIGURE 4C. Two-part Sika epoxy resin, comprising a

resin and hardener, mixed to a ratio of 1:1 was poured within the confines of the sheet pile upstands, 5mm below the crest, and was left to cure (FIGURE 4D). When pressing sheet piles into clay gaps formed at ground surface; the soil immediately adjacent the sheet pile group was pressed by hand against the pile to establish contact at the pile soil interface and a bead of grease was also applied to prevent the sample from drying out excessively.

Forming the solid circular piles was more complex and involved pre-cutting the pile bore. The circumference of the pile was etched using a scribe before a cutting guide was suspended above the model. Tubular cutters created a bore 60mm in diameter to a depth of 180mm before the base and edges of the bore were scraped clean. The smooth solid pile, 60mm in diameter, was carefully placed within the bore and the soil surface immediately adjacent the pile was pressed against the pile to ensure good contact between the soil and pile. The rough solid pile bore was achieved in a similar way, however the 60mm long plastic spacers protruding from the 48mmOD core ensured that the pile remained central whilst two-part Sika resin was poured in the void between the aluminium tube and soil and was cast level with the soil surface. It was not necessary to compress the soil around this pile as the resin was cast in-situ. Sand was poured into the tubular piles to ballast the pile and counter the effects of buoyancy.

Loading caps were placed on the piles before the loading frame was bolted onto the model. LVDTs, manufactured by Schlumberger and supplied by RS Components Ltd, Northants, were adjusted so that there was sufficient range of displacement and the loading beam was manually adjusted so that the load cells were at least two millimetres above the pile loading caps. Sub-miniature tension and compression 5kN Omega load cells (LCMFD series) were used to measure the pile behaviour in response to an applied load. This was to enable testing of the motor prior to spin up and ensure that it was functional. An overflow standpipe was connected to the base drain of the model to provide a water table 30mm below ground surface. The completed model on the centrifuge swing immediately prior to spin-up is given in FIGURE 4E.

General test scheme

The model was accelerated to 50g and was reconsolidated over a period of 24 hours. A PPT was monitored to determine whether the excess pore pressures had dissipated before the test was conducted.

The test involved lowering the loading beam at a rate of 1mm/minute which is generally accepted to represent undrained event in kaolin clay (ICE, 1997). Owing to the gap between the load cell pin and the pile loading cap an immediate response was not observed.

The data logger recorded load settlement data at one second intervals, which provided sufficient data for the rate at which the piles were loaded. The test continued until the measured displacement reached approximately 10% of the nominal pile diameter. Post-test shear vane readings were obtained in two locations to determine an average undrained shear strength profile to a depth of 250mm.

Summary of tests and results

Seven centrifuge experiments, each testing two piles, were conducted as part of the hybrid foundation study; a summary of each of the experiments are presented in TABLE 2 and a description is provided in this section. The results and back calculation of α are presented in TABLE 3.

- Test 1

A smooth solid pile was tested against a circular sheet pile (without perforations). This was the first in the test series and consequently this experiment primarily focussed on establishing suitable, repeatable and accurate model making techniques. Simple pile capacity analyses were conducted, as described in the next section, and the theoretical base capacity exceeded the total measured pile capacity by a factor of 1.75. The solid tubular pile became buoyant as

the tube had not been ballasted. The load/displacement response is plotted in FIGURE 5A showing that the sheet pile generated greater capacity, owing to the solid pile buoyancy effects.

- Test 2

This test modelled a rough solid pile against a circular sheet pile (without perforations). This test realistically modelled a concrete pile with a surface roughness that could be considered reasonably representative of the prototype. The pile became buoyant during in-flight consolidation as it had not been ballasted to mitigate the soil that had been bored and may have affected the capacity of the pile. Back calculation of α was found to be 0.48, which was reasonable for the strength of soil. Comparisons between the magnitude and trend of the circular sheet pile in tests 1 and 2 (FIGURE 5B) were evident, indicating reliability in the circular sheet pile results.

- Test 3

A ballasted smooth solid pile and a perforated circular sheet pile were loaded simultaneously to investigate the influence of perforations on the capacity of a circular sheet pile group. To facilitate this, 5mm diameter holes were drilled at 30mm centres along the inner ribs of the existing circular sheet pile, visible in FIGURE 3. The perforations increased the capacity of the sheet pile by a factor of two at working load and increased the ultimate pile capacity by approximately 50%, see FIGURE 5C. The capacity generated by the smooth solid pile was similar to the perforated sheet pile at 1% normalised settlement but a marginally lower ultimate capacity.

- Test 4

The perforated circular sheet pile was tested against a conventional circular rough solid shafted concrete pile in this test. The sheet pile load cell was unresponsive so comparisons were drawn between the rough solid pile and the Test 3 perforated circular sheet pile, shown in FIGURE 5D.

- Test 5

At this stage, comparisons had already been established between the circular sheet piles, with and without perforations. Test 5 was conducted to compare and quantify sheet pile capacity against a conventional solid concrete circular shafted pile (test 4). A square sheet pile was modelled to measure the influence of geometry on pile capacity. Centrifuge operational problems were encountered shortly after spin-up so it was necessary to test the piles immediately without reconsolidating the sample. The results are presented in FIGURE 5E alongside the rough solid pile (test 4) and the perforated circular sheet pile (test 3). Both rough solid piles converged towards similar capacities, however a peak was observed at 2% normalised settlement. It is likely that this occurred as excess pore pressures had not dissipated and the piles were subsequently tested in undrained conditions. The load settlement trend attributed to the square sheet pile was consistent with the perforated circular sheet pile with 40% increase in capacity.

- Test 6

Further investigations into the influence of sheet pile geometry and shaft area on bearing capacity were carried out with a small square sheet pile. Four individual narrow sheets of corrugated plate were welded together to form the sheet pile. The nominal width of the small sheet pile was 43mm, giving a perimeter of 214mm, comparable with the circular sheet pile, see TABLE 2. The small and large square sheet piles were tested together and the results are presented in FIGURE 5F.

The behaviour of a circular sheet pile, with and without perforations, (tests 2 and 3) are also plotted for comparison. Comparable pile surface areas generated similar bearing capacities. This demonstrates that hybrid piles are governed by shaft friction as opposed to end bearing owing to the plug of soil contained within the sheet piles.

- Test 7

Test 7 was designed as a repeat test to validate the results of the large square sheet pile and the perforated circular sheet pile. Whilst the model reconsolidated in-flight the square sheet pile load cell became unresponsive. The results of the perforated circular sheet pile are presented in FIGURE 5G and are compared with the behaviour observed in test 3. Although the capacity in test 7 was 30% greater than that measured in test 3, the general pile responses are comparable.

Analysis

Previous analyses used the simple Terzaghi pile capacity theory (equations 1 – 3) to back analyse the values of α (Panchal *et al*., 2016).

$$Q_{ult} = Q_b + Q_s \quad (1)$$

$$Q_s = A_s \alpha S_u \quad (2)$$

$$Q_b = [A_b(N_c S_u + \gamma H)] \quad (3)$$

$$Q_b = {}^{[A_b(N_c S_u + \gamma H)]}/_{2} \quad (4)$$

However, it was later appreciated that owing to the resin pile cap that had been cast at ground level a degree of plugging within the sheet pile group could influence the overall pile capacity. The base capacity was reduced by a factor of two in compliance with the ICP design standards for open ended tubular piles (Jardine *et al*., 2005) which gave equation (4). The bearing capacity factor (N_c) of long slender piles was taken as 9, however the D/B ratios ranged from 3.0 to 4.1, therefore N_c factors range from 8.8 to 9.0. The small variation in N_c was shown to have little influence on the computed values of α. Back analyses of α using the ICP open ended tubular pile method are presented in TABLE 1, whilst a summary of the computed α values are given in TABLE 4.

TABLE 3 demonstrates consistency between the back analysed values of α for the rough solid piles. However, notable variation exists between α values for large square sheet piles, with test 5 presenting an α value 40% greater than that determined from test 6. Similarly, the

difference between α values for the perforated sheet piles, in tests 3 and 7 are also dissimilar by 40%.

At first glance, the pile capacities generated across this series of tests seem wide ranging. However, there were variations in soil strengths, with averages ranging from 42-51kN/m^2, see TABLE 1. Direct comparisons between tests was made by normalising the axial loads against the average undrained shear strengths along the length of the piles. FIGURE 6A illustrates the influence of perforations on the capacity of sheet piles, in addition to the surface roughness of a solid pile. All piles exhibited similar responses during initial loading, however as the piles approached working load the benefits of perforations were notable. Perforations resulted in 75% increase in the capacity of an unperforated circular sheet pile and a similar response to a rough solid circular pile.

Pile geometry was shown to have a significant impact on the capacity of a sheet pile group. FIGURE 6B demonstrates that whilst the base areas of the square and circular sheet piles were comparable, increasing the shaft area by 13% could as much as double the capacity of the sheet pile group. The square sheet pile group also gave a stiffer response at the initial stages of loading compared with the rough solid or circular sheet piles.

Having established that square sheet piles offer a considerable increase in pile capacity, FIGURE 6C compares the performance of small and large square sheet piles. The base and shaft areas of the small square sheet pile were 45% and 15% less than the large sheet pile respectively, resulting in a 52% reduction in capacity.

Discussion

At first glance the rough solid circular pile α values may be considered low. However, this is typical for model piles cast in place owing to the relatively smooth condition of the bore, compared with the surface achieved through rotary or CFA piling. The pre-bore was formed using sharpened tubular cutters, which produced a relatively smooth bore, shown in FIGURE 7A, and subsequently the surface of resin pile was not excessively rough, as illustrated in

FIGURE 7B. The interaction between the resin pile and bore was not representative of a concrete pile, which should, in theory, be approximately 0.5 for soil strengths in the region of 50kN/m^2, as predicted using FIGURE 8 (Huang & Yu, 2018). In-flight undrained shear strength measurements are usually taken, however a Pilcon hand shear vane was used in this series of tests. S_u readings using the hand shear vane tend to be more linear and slightly higher than those measured in-situ using an actuated T-bar (Gorasia & McNamara, 2016), all measurements were taken at similar instances for all models. The consistency between S_u readings demonstrates that the piles were loaded in similar strengths of soil.

A bead of silicone grease was applied around the edge of the strong tub to prevent the sample from drying out whilst in-flight. In the initial series of tests grease had also been applied around the edges of the sheet piles as a gap between the pile and soil had formed as the sheet pile was embedded in the soil, as shown in FIGURE 9A. However, when the model was accelerated the grease seeped down the gap as the sample reconsolidated, forming a barrier between the soil and pile close to the pile head visible in FIGURE 9B. Consequently, the lubricated sheet piles reduced the soil-pile adhesion resulting in reduced pile capacity. Silicone grease was not used to seal the gap that had formed between the sheet piles and soil in test 7; consequently, this resulted in a higher α value and higher capacity.

Although square sheet pile in test 7 provided no results examination of the α values obtained from test 6, where two square sheet piles were modelled, gave comparable α values. Both sheet piles were formed from the same material so it is reasonable to suggest that similar α values should be obtained. This lends some validity to the results obtained in test 6 and consequently the α value of a square sheet pile can be expected to be in the region of 0.5-0.6.

Arguably, similar α values should be obtained for any sheet pile geometry, provided they are formed from the same material and subsequently have equivalent surface roughness. However, the unperforated square sheet piles gave α values two times greater than the circular sheet piles. Variations in α may be owing to the width of the re-entrant spacing

between the sheet pile ribs, as demonstrated in FIGURE 10. Both sheet piles were formed from a single corrugated sheet; the square was formed by folding and crimping the corners whilst maintaining relatively parallel sides, however the circle was formed by rolling the sheet. This fabrication process resulted in variations in the rib spacing width between the two sheet pile geometries. Narrower rib (re-entrant) spacing resulted in a greater degree of plugging between the pile ribs. However, the full scale prototype individual sheet piles would be installed to form the required geometry. Therefore, the re-entrant spacing would be comparable for a range of sheet pile group geometries, resulting in comparable plugging effects and ultimately α values.

Boundary effects from the positioning of the piles in the centrifuge strong tub were deemd to be negligible based on the literature published by Ullah et al. (2016). The studies demonstrated that boundary effect zones in uniform clay samples are negligible where L/D is greater than or equal to 2. Furthermore, Ullah et al. predict possible boundary effects exist where the ratio ranges between 2 and 1.5 and ratios less than 1.5 suggest boundary effects are prominent. The worst case L/D ratio for this series of tests equated to 1.8 between the piles and the edge of the strong tub. Considering the α values that had been achieved the piles can be considered smooth, which according to Ullah et al. further reduces the influence of boundary effects.

Whilst efforts were made to maintain sheet pile verticality during installation, some degree of misalignment was often occurred, therefore as the pile was loaded the LVDTs showed one side of the pile being loaded more rapidly as the test progressed; as shown in FIGURE 11A, illustrative of the measurements taken in test 5. This resulted in eccentric loading of the pile which contributed to a reduced pile bearing capacity, which was particularly evident in sheet pile tests, as illustrated in FIGURE 11B.

Sika Biresin was used in these tests which comprised a two-part resin and hardener. This was a suitable material as it was mixed immediately before use and rapidly cured; a filler, however, was not used. Fillers are typically added to resins to reduce the effects of shrinkage

and curing exotherm. For the sheet piles this was considered to have a minimal effect on the overall performance, as the resin was cast above ground surface. However, the exothermic reaction may have influenced the behaviour of the rough circular solid shafted pile owing to the large area of contact between the resin and soil. The moisture that had evaporated as the resin cured may have been replenished by the water table as the sample reconsolidated in-flight. However, the similarity of results and computed α values suggest that although the rough solid piles may have been affected by shrinkage and exothermic processes, there was a high degree of internal consistency between tests.

The large square sheet pile foundation was dimensionally similar to the circular sheet pile, as indicated in TABLE 2, although the measured perimeters of the solid and sheet pile shafts were significantly difference. Therefore, the square sheet pile mobilised a higher proportion of shaft friction, resulting in an improved bearing capacity at both the working load and ultimate load of the pile.

Conclusion and further work

A total of seven centrifuge tests have been conducted at 50g to investigate the merits of the hybrid pile compared with a conventional solid circular shafted concrete pile. Each experiment tested two model piles up to 60mm in diameter and 180mm long, representative of a 3m in diameter and 9m in length at prototype scale. Two pile types were tested; solid shafted piles and sheet pile groups. Variations of the solid shafted pile included smooth and rough piles whilst circular and square sheet pile geometries were modelled. The influence of perforations along the sheet pile shaft was also explored.

The hybrid foundation solution offers a competitive and sustainable alternative to conventional solid concrete piles. Where the basal areas of a sheet pile group and solid circular pile are equal, comparable capacities were obtained. The capacity of the sheet pile was shown to be highly sensitive to rib spacing, with a square arrangement offering double the capacity of a

circular sheet pile, whilst the difference in shaft area was less than 15%. Perforations along the sheet pile group shaft have been demonstrated to increase capacity by up to 40%, owing to the additional soil-soil shearing interfaces.

It is widely accepted that piles transfer load through a combination of end bearing and shaft friction, however, in clay soils most of the load is transferred through skin friction at lower depths, owing to greater undrained shear strengths. Tests modelling sheet piles partially perforated along lower portions of the sheet piles should be undertaken to establish whether similar capacities can be achieved for completely perforated sheet piles and optimise axial capacity of the sheet piles and perforations.

References

Bransby, M.F. & Yun, G.-J., 2009. The undrained capacity of skirted strip foundations under combined loading. Geotechnique, 59(2), pp.115-125.

Gorasia, R.J., 2013. Behaviour of ribbed piles in clay. *PhD thesis*, City, University of London, UK.

Gorasia, R.J., McNamara, A.M., 2016. High-capacity ribbed pile foundations. *Proceedings of the Institution of Civil Engineers - Geotechnical Engineering,* 169(3), pp. 264-275.

Huang, A.-B. & Yu, H.-S., 2018. Foundation engineering analysis and design, Taylor & Francis, UK.

Institution of Civil Engineers, 1997. Specification for piling and embedded retaining walls, (1st edn) Thomas Telford, London

Jardine, R., Chow, F., Overy, R. & Standing, J., 2005. 4 Design Methods for Piles in Clay. ICP design methods for driven piles in sands and clays. January 2005, Thomas Telford, London, pp. 28-37.

O'Brien, A.S., 2012. Chapter 52 Foundation types and conceptual design principles. *ICE manual of geotechnical engineering*: Volume II. pp. 733-764.

Panchal, J.P. McNamara, A.M.M & Goodey, R.J., 2016. Bearing capacity of sheet piled foundations. *In Proceedings of 2nd Asian Conference on Physical Modelling in Geotechnics*, Shanghai, China, pp. 1-6.

Panchal, J.P. McNamara, A.M.M & Goodey, R.J., 2018a. Influence of geometry on the bearing capacity of sheet piled foundations. *In Proceedings of 9th International Conference on Physical Modelling in Geotechnics*, London, UK, pp. 1395- 1400.

Panchal, J.P. McNamara, A.M.M & Goodey, R.J., 2018b. Centrifuge modelling on the influence of size and geometry of hybrid foundations on bearing capacity. *In Proceedings of 1st International Conference on Press-in Engineering*, Kochi, Japan.

Terzaghi, K., 1943. Theoretical Soil Mechanics, John Wiley & Sons, New York, USA

Ullah, S.N., Hu, X., Stanier, S. and White D. (2016) Lateral boundary effects in centrifuge foundation tests. International Journal of Physical Modelling in Geotechnics, 17(3), pp. 144-160

FIGURES

Figure 1: Cross section of model in centrifuge strongtub

Figure 2: Detailed cross sections through model piles (a) rough solid pile and (b) typical sheet pile hybrid foundation

Figure 3: Photographs of model piles used in experiments

Figure 4: Model making stages (a) trim sample (b) mark out pile centres (c) embed sheet piles using hydraulic press (d) cast resin pile caps (e) model immediately prior to spin-up

Figure 5: Test results (a) test 1; smooth solid and circular sheet pile (b) test 2; rough solid and circular sheet pile (c) test 3; smooth solid and perforated circular sheet pile (d) test 4; rough

solid (e) test 5; rough solid and large square sheet pile (f) test 6; large and small square sheet piles and (g) test 7; perforated circular sheet pile

FIGURE 6: Axial loads normalised against average undrained shear strength illustrating the influence of perforations, influence of sheet pile geometry and influence of dimensions of square sheet piles on load-settlement behaviour

FIGURE 7: Photographs taken looking down on sample of (a) relatively smooth pre-bore for modelling solid shafted piles prior to installation of pile and (b) rough pile exhumed from sample

FIGURE 8: Estimate of α value (Huang & Yu, 2018)

FIGURE 9: Photograph of (a) gap immediately adjacent sheet pile in previous tests and (b) exhumed sheet pile post-test showing consolidation of clay around bottom third of sheet pile

FIGURE 10: Influence of re-entrant spacing on shear zone and *α* values (after Panchal *et al*., 2018b)

FIGURE 11: Effect of eccentric loading on large square sheet pile in test 5 (a) LVDT readings and (b) photograph of sheet pile post test

Figure 1

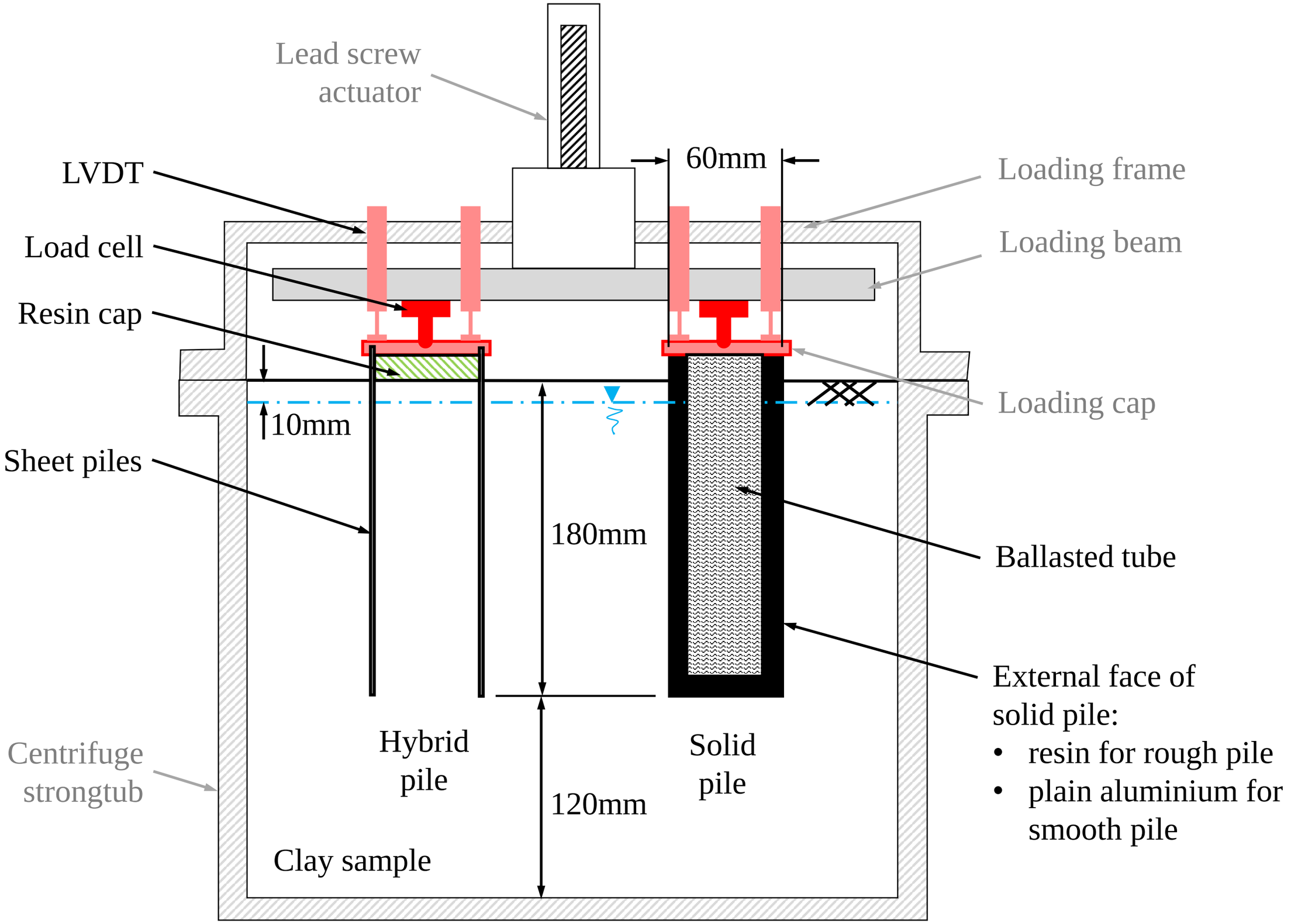
Lead screw actuator
LVDT
Load cell
Resin cap
60mm
Loading frame
Loading beam
Loading cap
10mm
Sheet piles
180mm
Ballasted tube
External face of solid pile:
• resin for rough pile
• plain aluminium for smooth pile
Centrifuge strongtub
Hybrid pile
Solid pile
120mm
Clay sample

Figure 2A – Solid pile

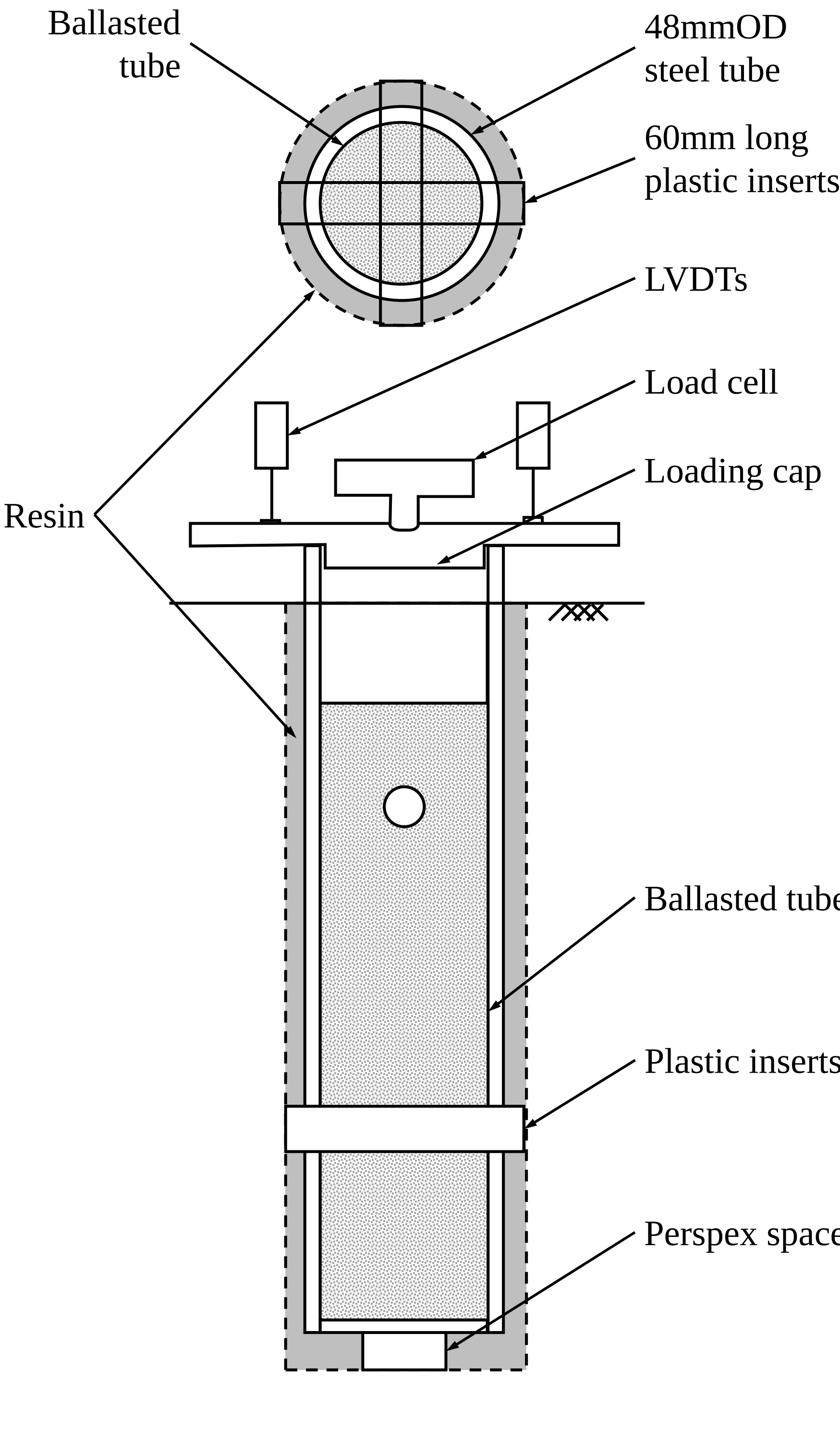

Figure 2B – Sheet pile

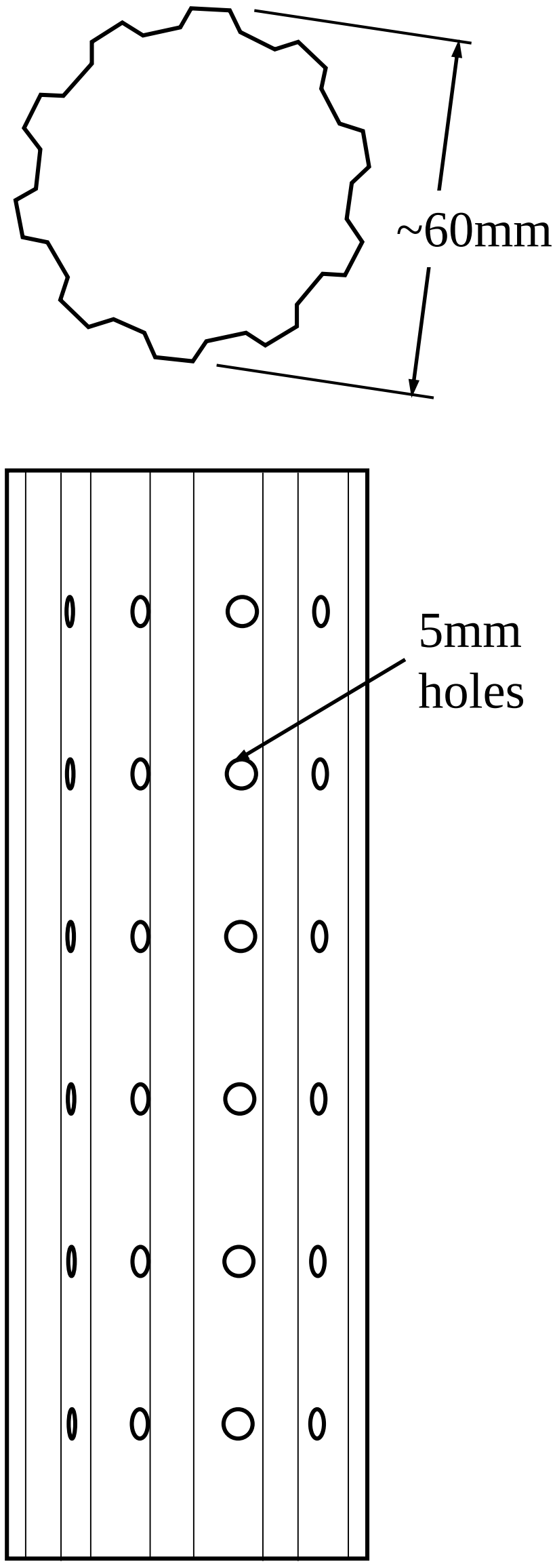

(a)

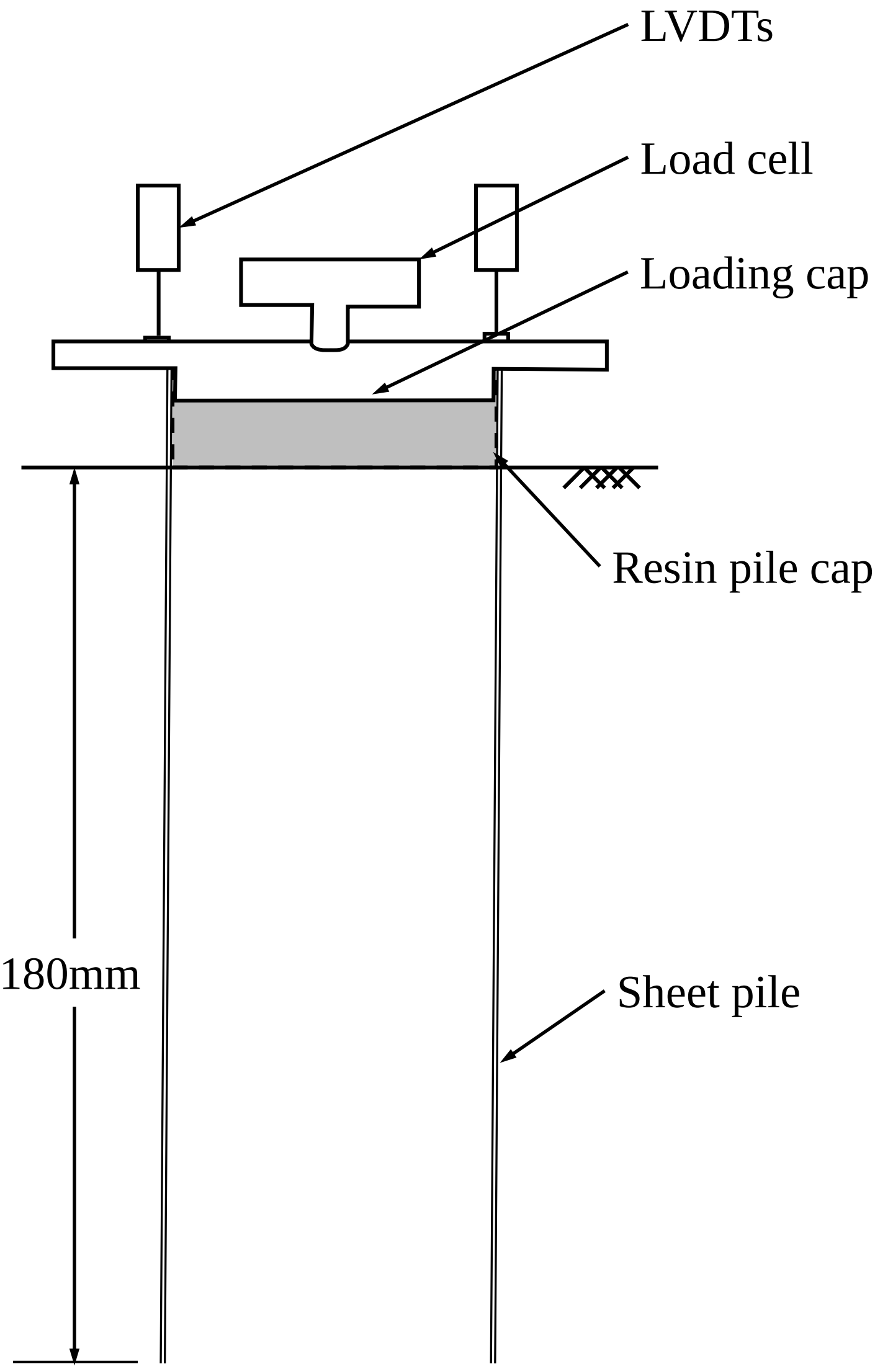

(b)

Figure 3

FIGURE 3

Large square sheet pile

Small square sheet pile

Smooth solid pile

Perforated circular sheet pile

Rough solid pile

Figure 4a

Click here to access/download;Figure;FIGURE 4A.jpg

Figure 4b

Click here to access/download;Figure;FIGURE 4B.JPG

Figure 4c

Click here to access/download;Figure;FIGURE 4C.JPG

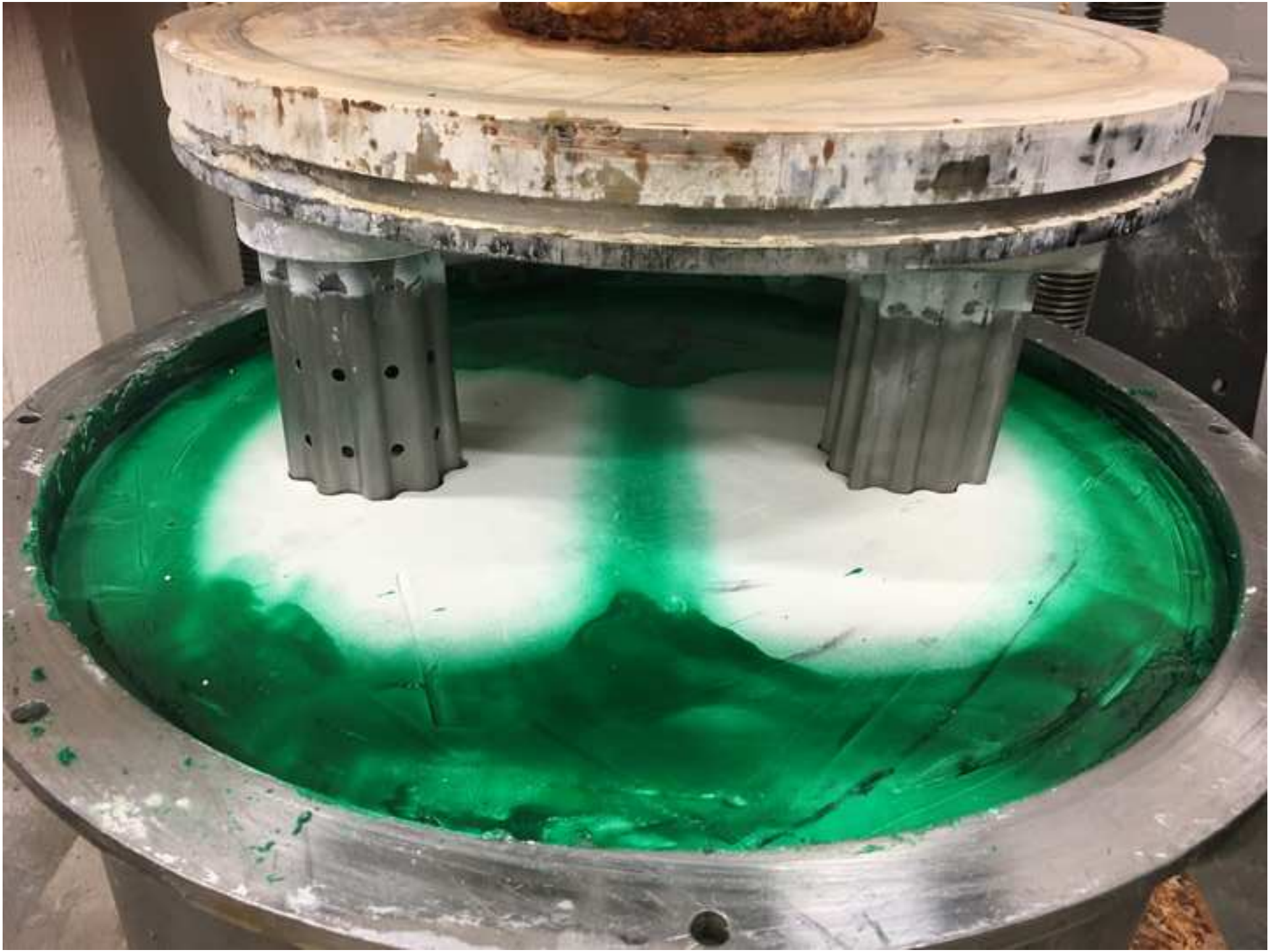

Figure 4d

Click here to access/download;Figure;FIGURE 4D.JPG

Figure 4e

Click here to access/download;Figure;FIGURE 4E.JPG

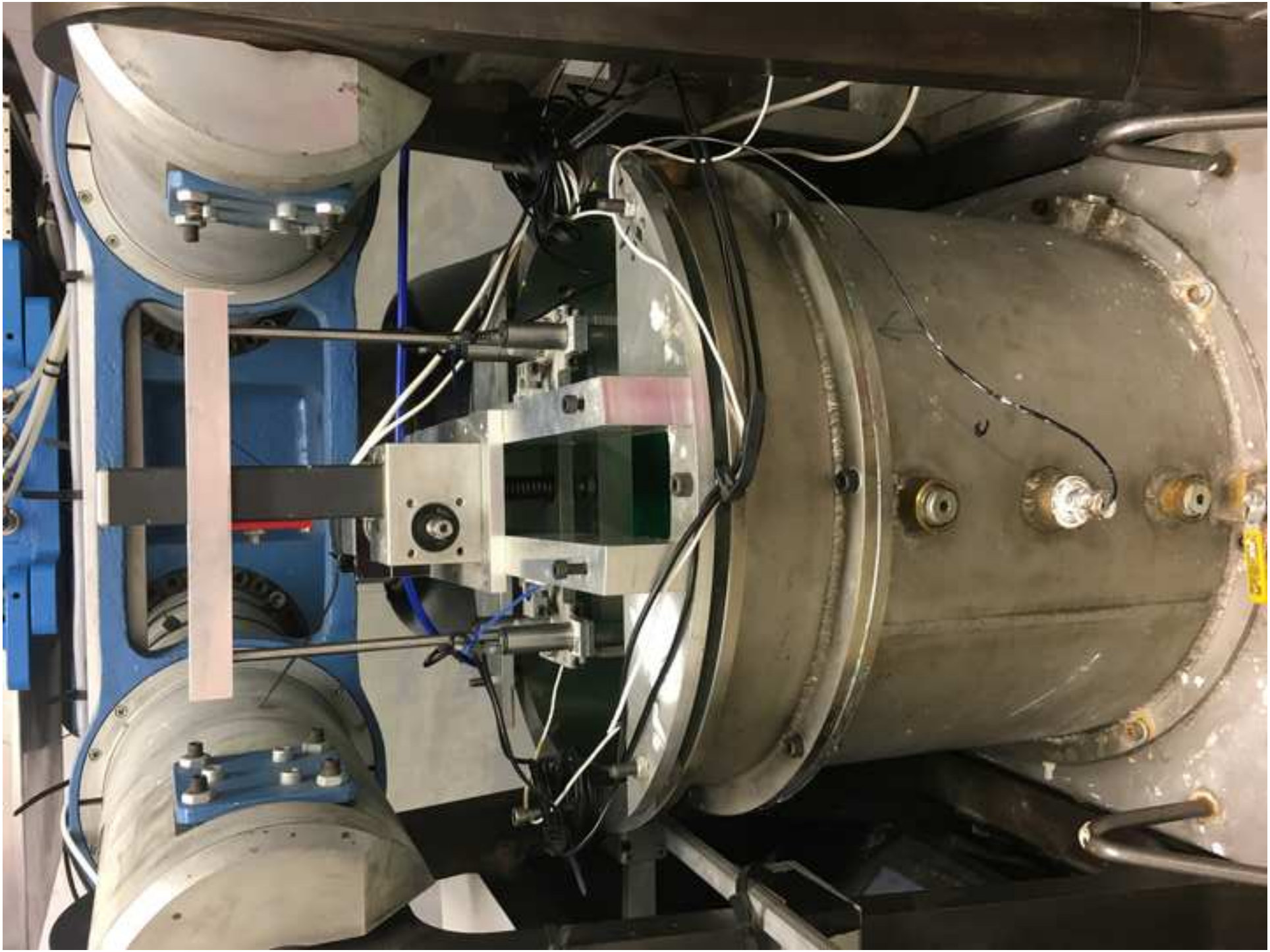

Figure 5

5A

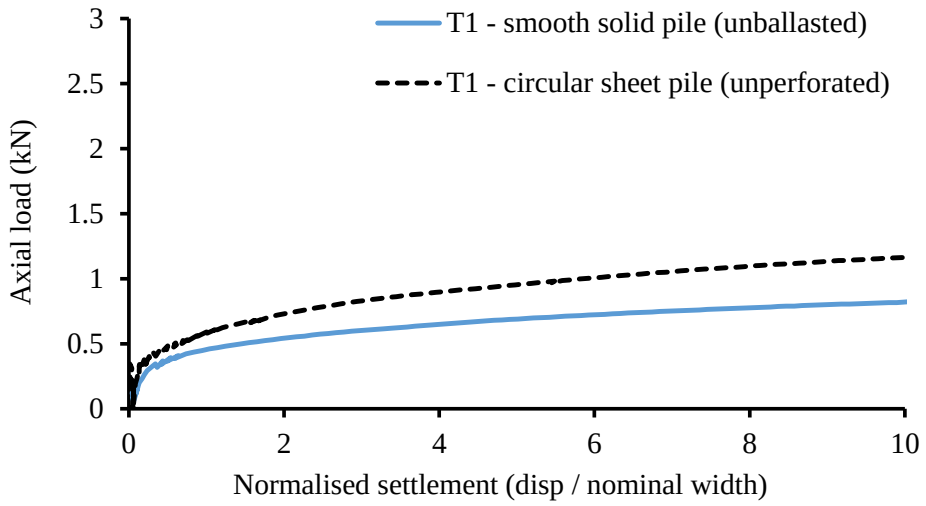

5B

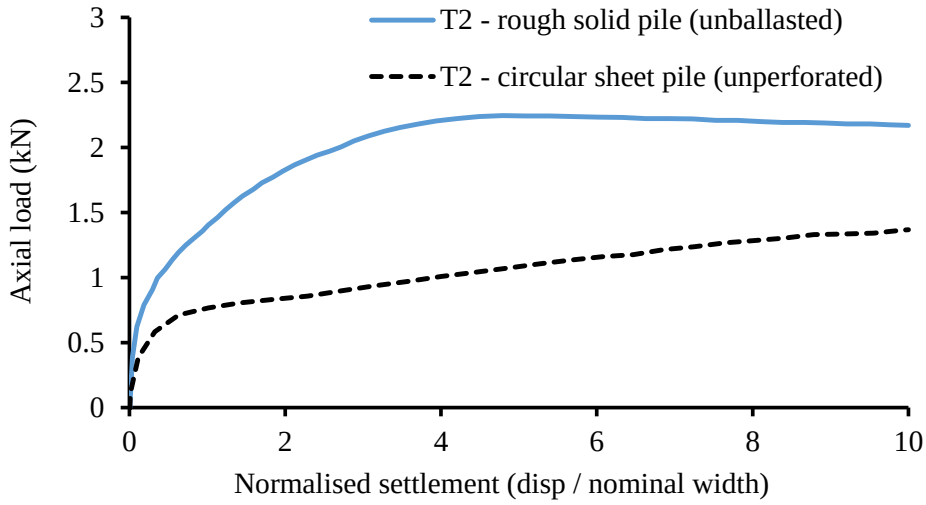

5C

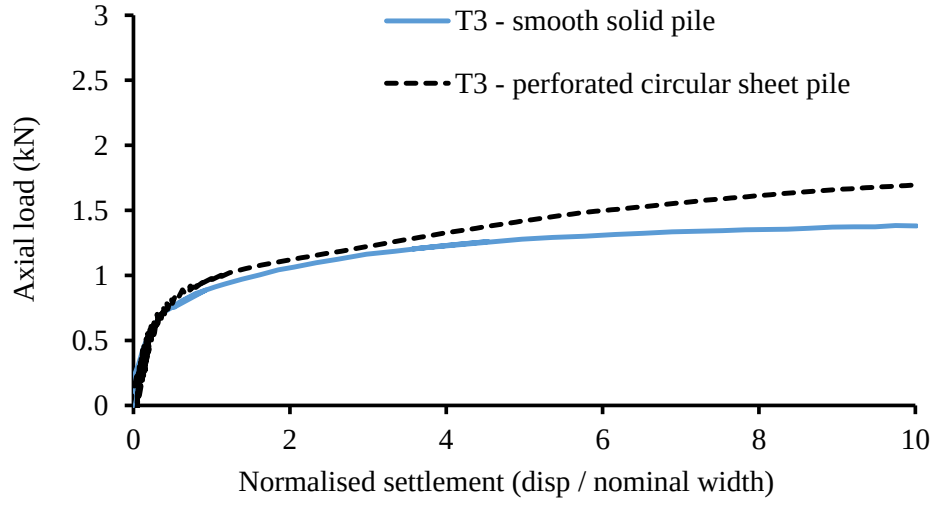

5D

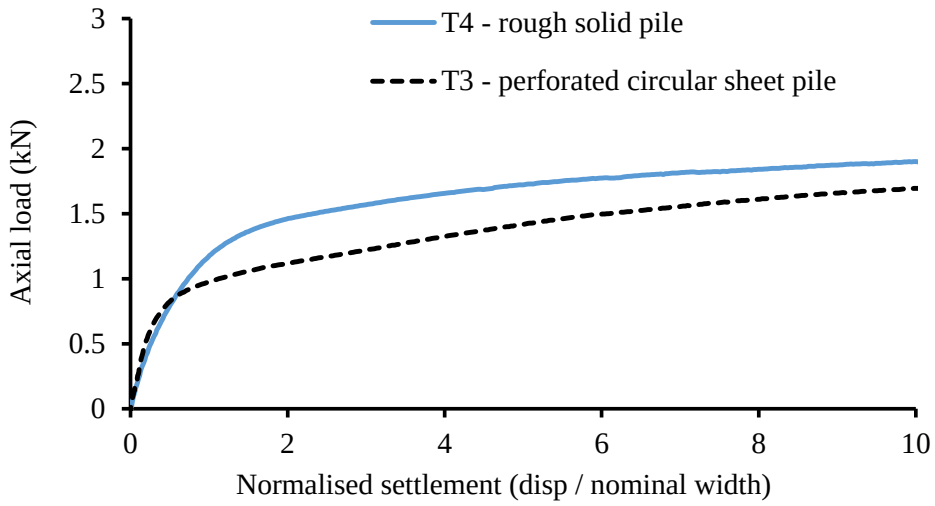
T4 - rough solid pile
T3 - perforated circular sheet pile
Axial load (kN)
Normalised settlement (disp / nominal width)
0
0.5
1
1.5
2
2.5
3
0
2
4
6
8
10

5E

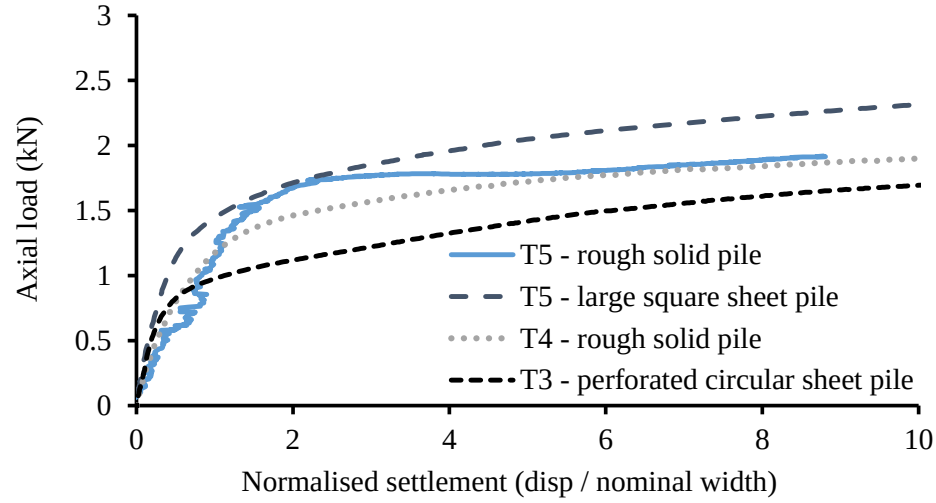
T5 - rough solid pile
T5 - large square sheet pile
T4 - rough solid pile
T3 - perforated circular sheet pile
Axial load (kN)
Normalised settlement (disp / nominal width)
0
0.5
1
1.5
2
2.5
3
0
2
4
6
8
10

5F

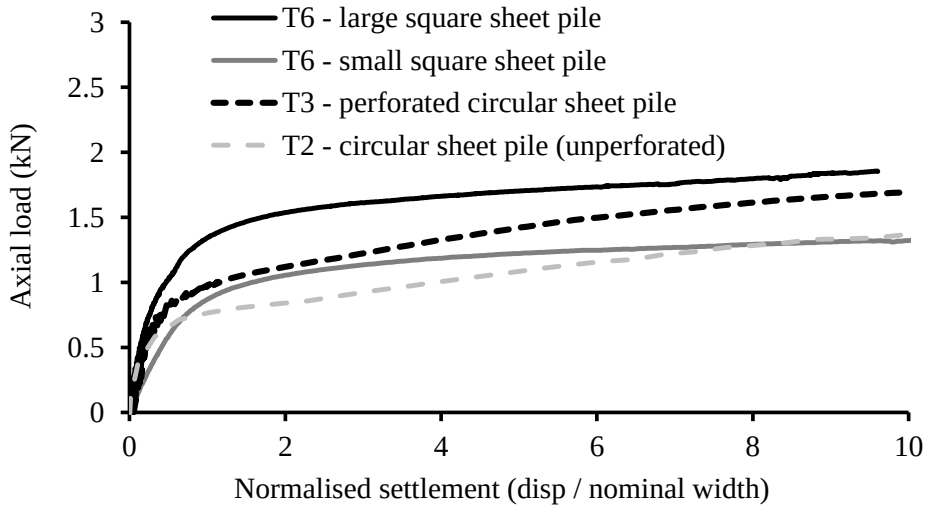
T6 - large square sheet pile
T6 - small square sheet pile
T3 - perforated circular sheet pile
T2 - circular sheet pile (unperforated)
Axial load (kN)
Normalised settlement (disp / nominal width)
0
0.5
1
1.5
2
2.5
3
0
2
4
6
8
10

5G

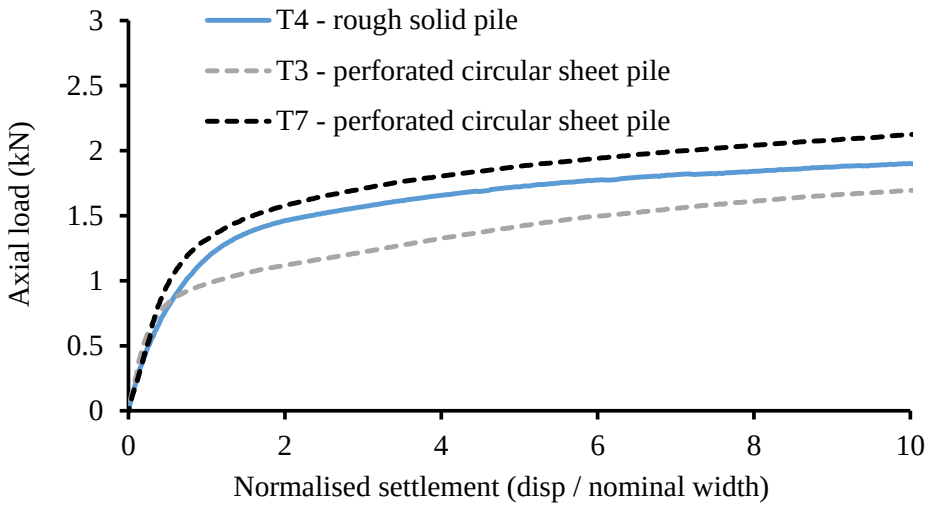
T4 - rough solid pile
T3 - perforated circular sheet pile
T7 - perforated circular sheet pile
Axial load (kN)
3
2.5
2
1.5
1
0.5
0
0
2
4
6
8
10
Normalised settlement (disp / nominal width)

Figure 6

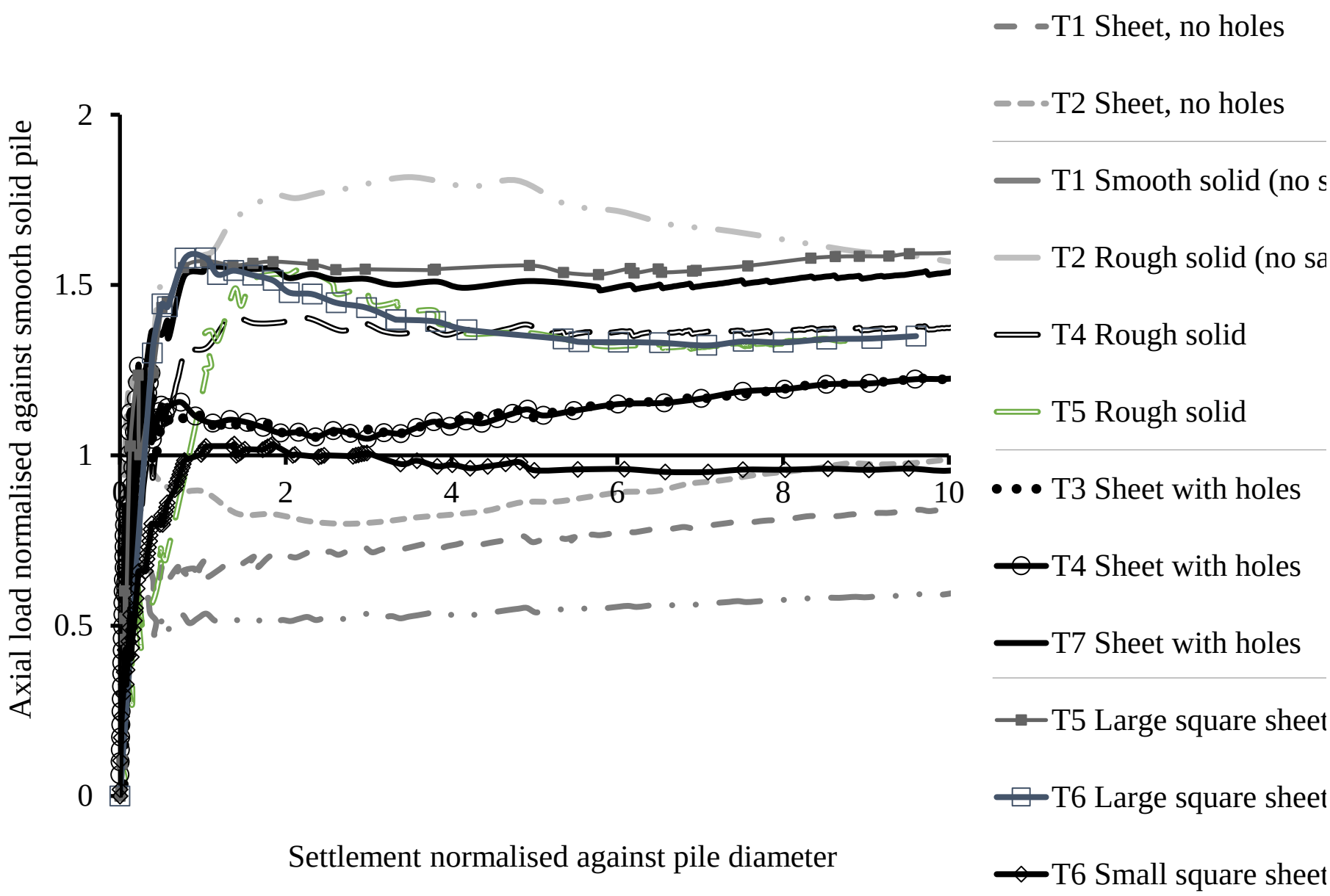
Axial load normalised against smooth solid pile
2
1.5
1
0.5
0
0
2
4
6
8
10
Settlement normalised against pile diameter
T1 Sheet, no holes
T2 Sheet, no holes
T1 Smooth solid (no s
T2 Rough solid (no sa
T4 Rough solid
T5 Rough solid
T3 Sheet with holes
T4 Sheet with holes
T7 Sheet with holes
T5 Large square sheet
T6 Large square sheet
T6 Small square sheet

Figure 7

FIGURE 7A

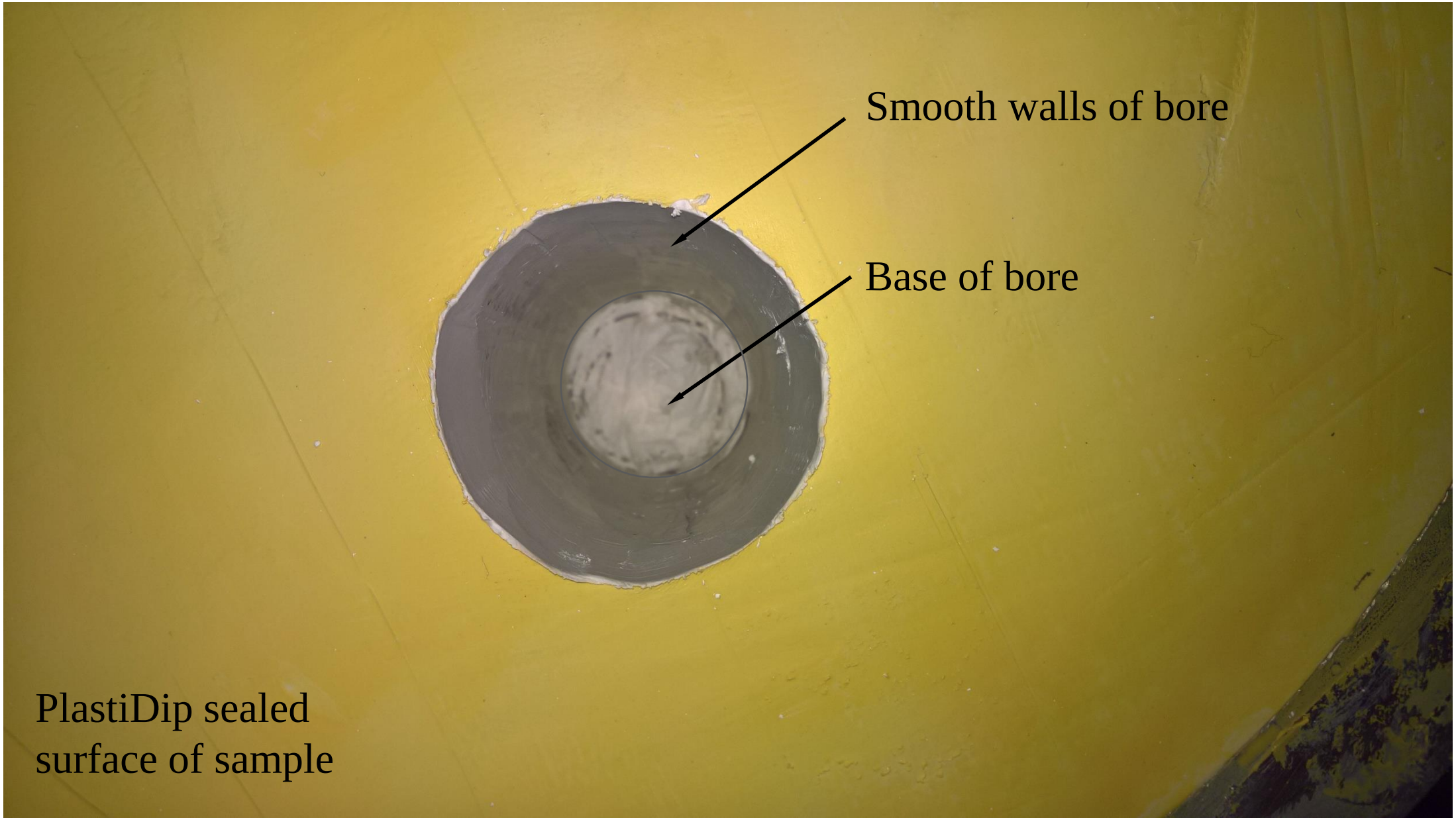

FIGURE 7B

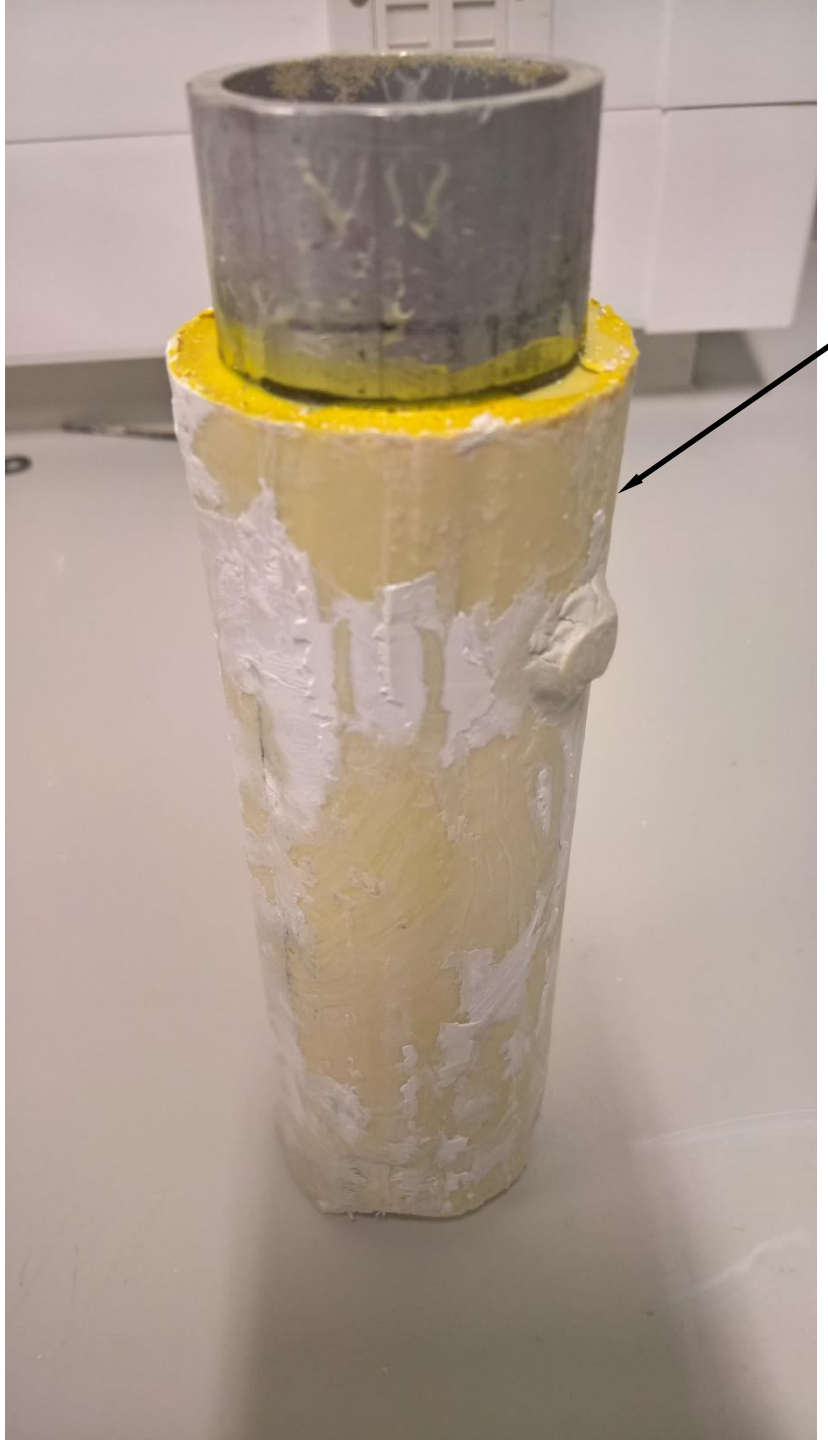

Relatively smooth resin pile modelling a “rough” concrete pile

Figure 8

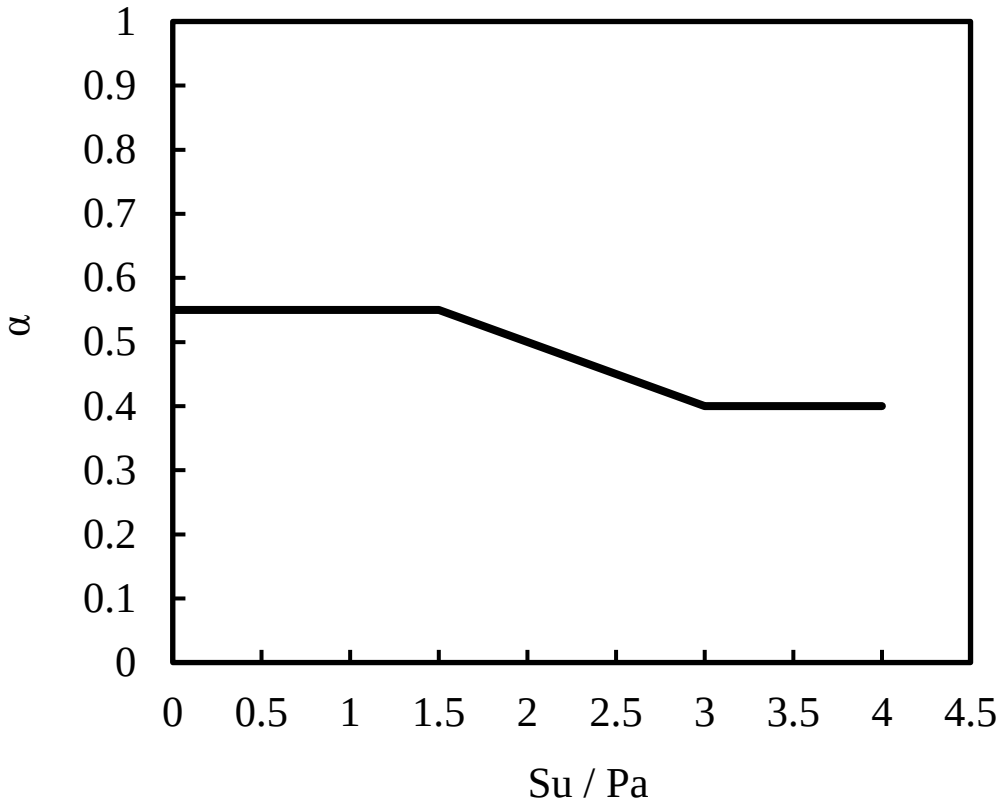

Figure 9a

Click here to access/download;Figure;FIGURE 9A.jpg

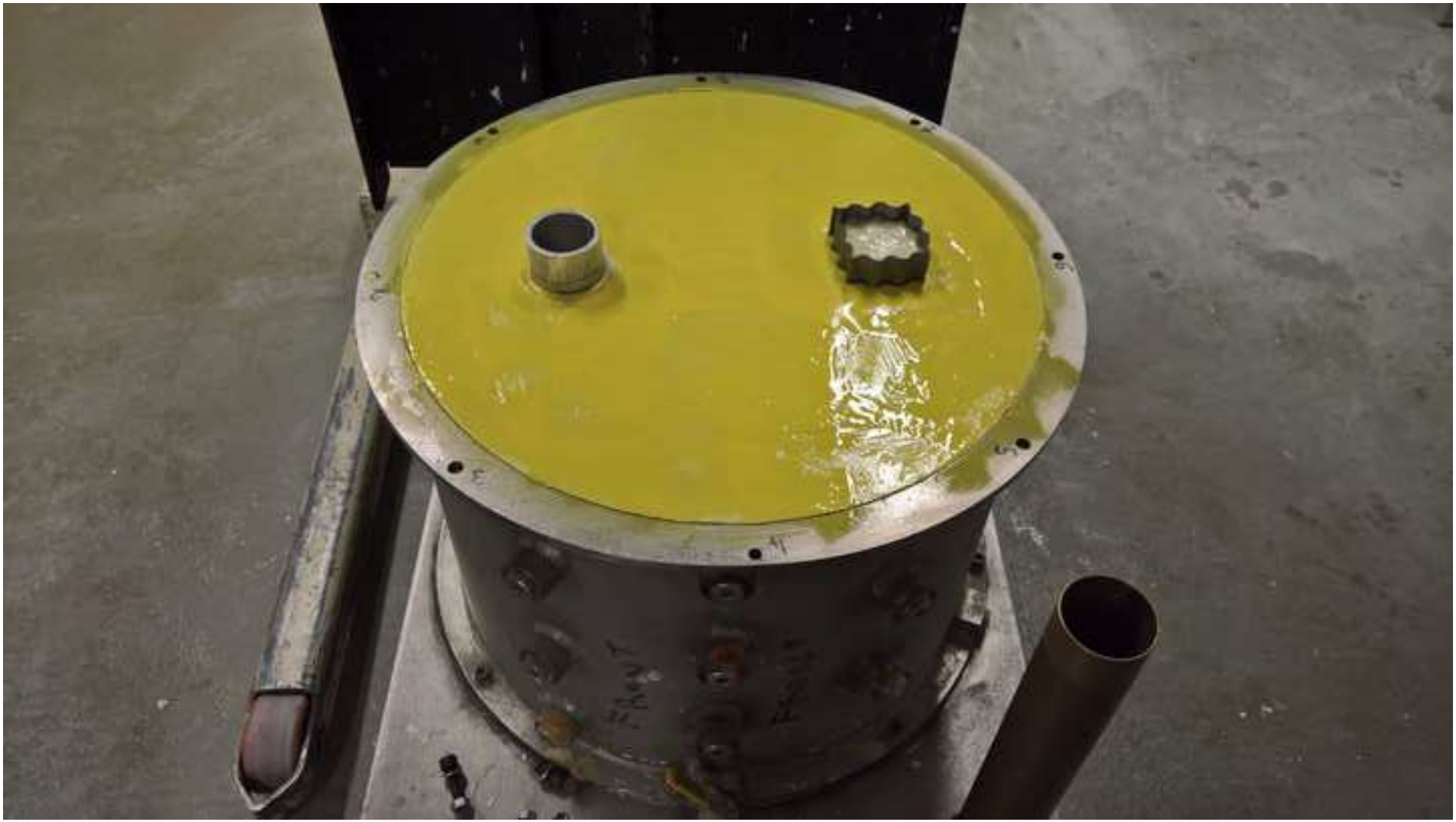

Figure 9b

Click here to access/download;Figure;FIGURE 9B.jpg

Figure 10

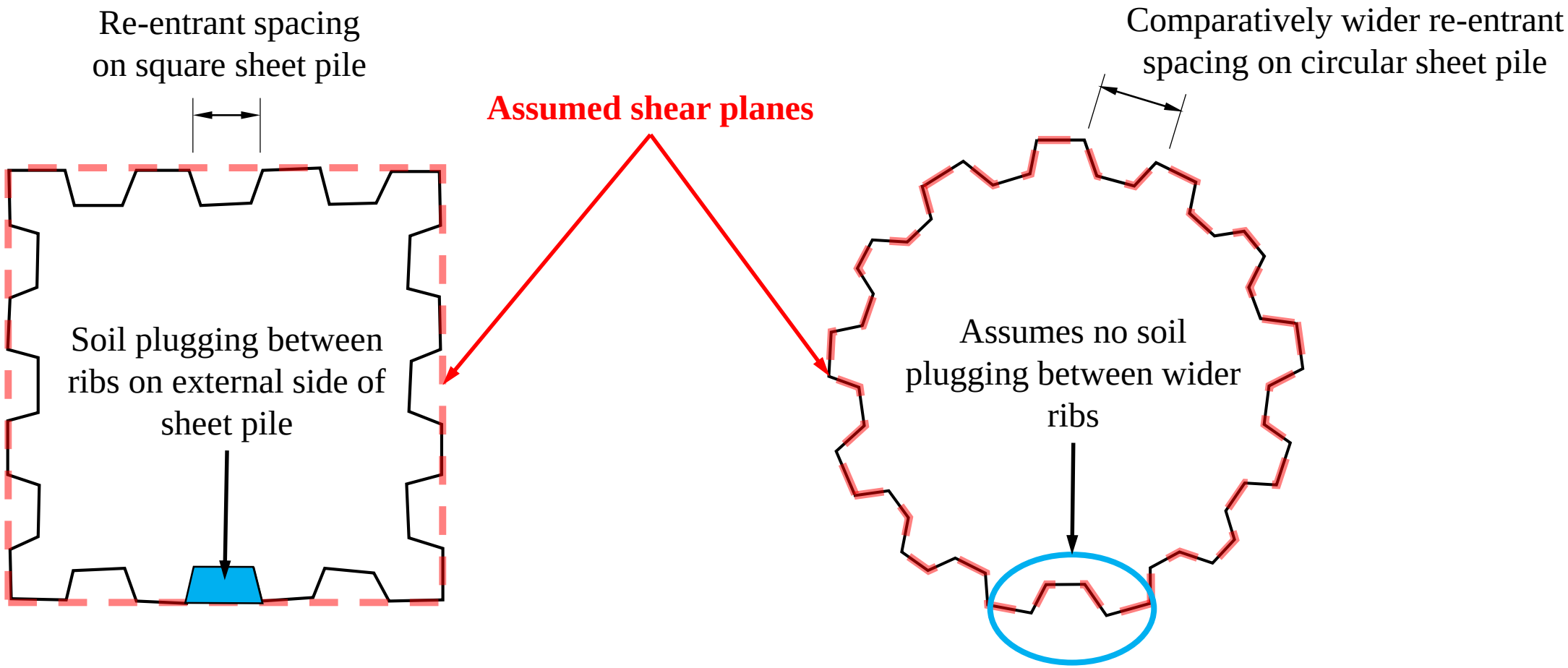
Re-entrant spacing
on square sheet pile
Assumed shear planes
Comparatively wider re-entrant
spacing on circular sheet pile
Soil plugging between
ribs on external side of
sheet pile
Assumes no soil
plugging between wider
ribs

Figure 11

FIGURE 11A

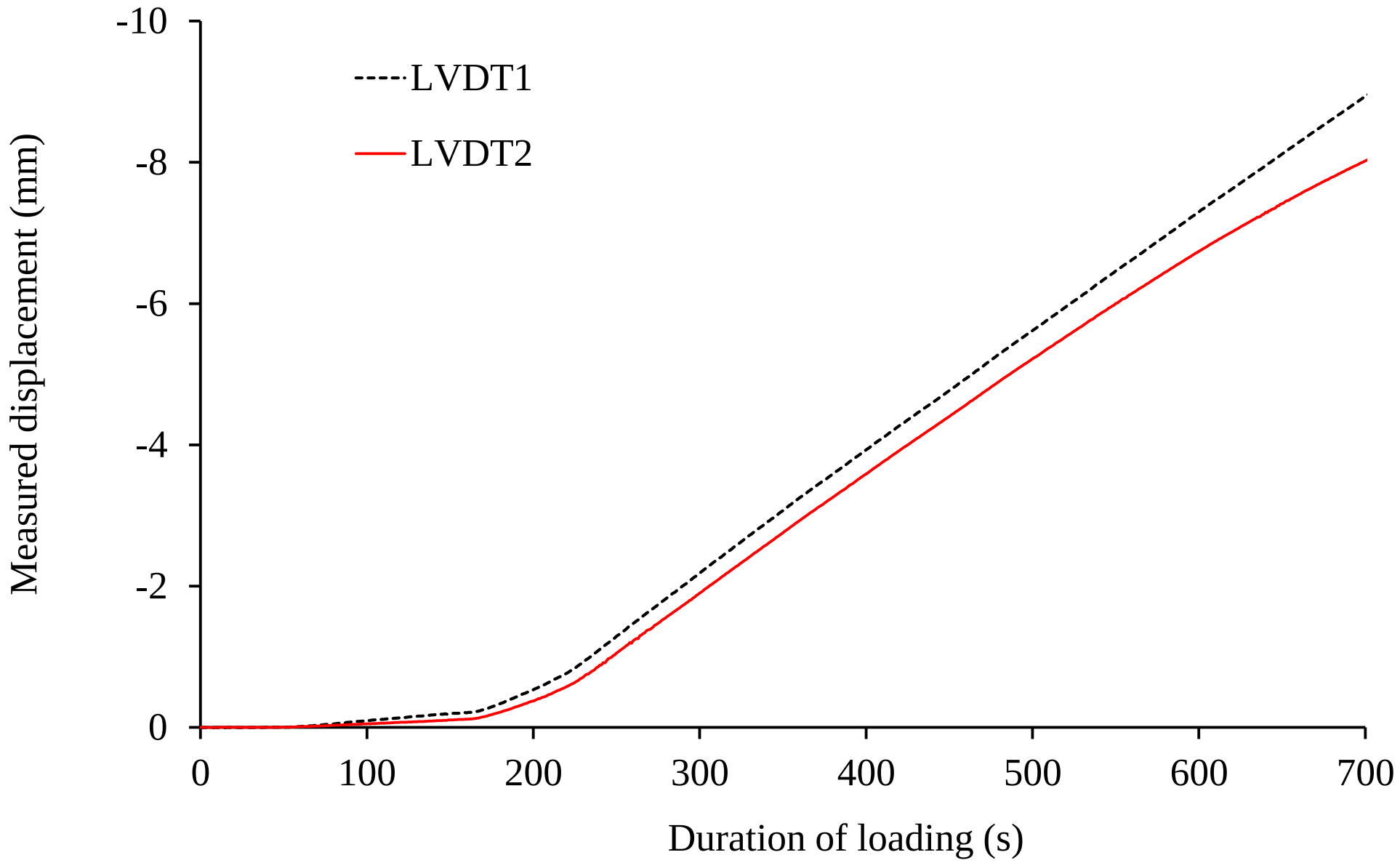

FIGURE 11B

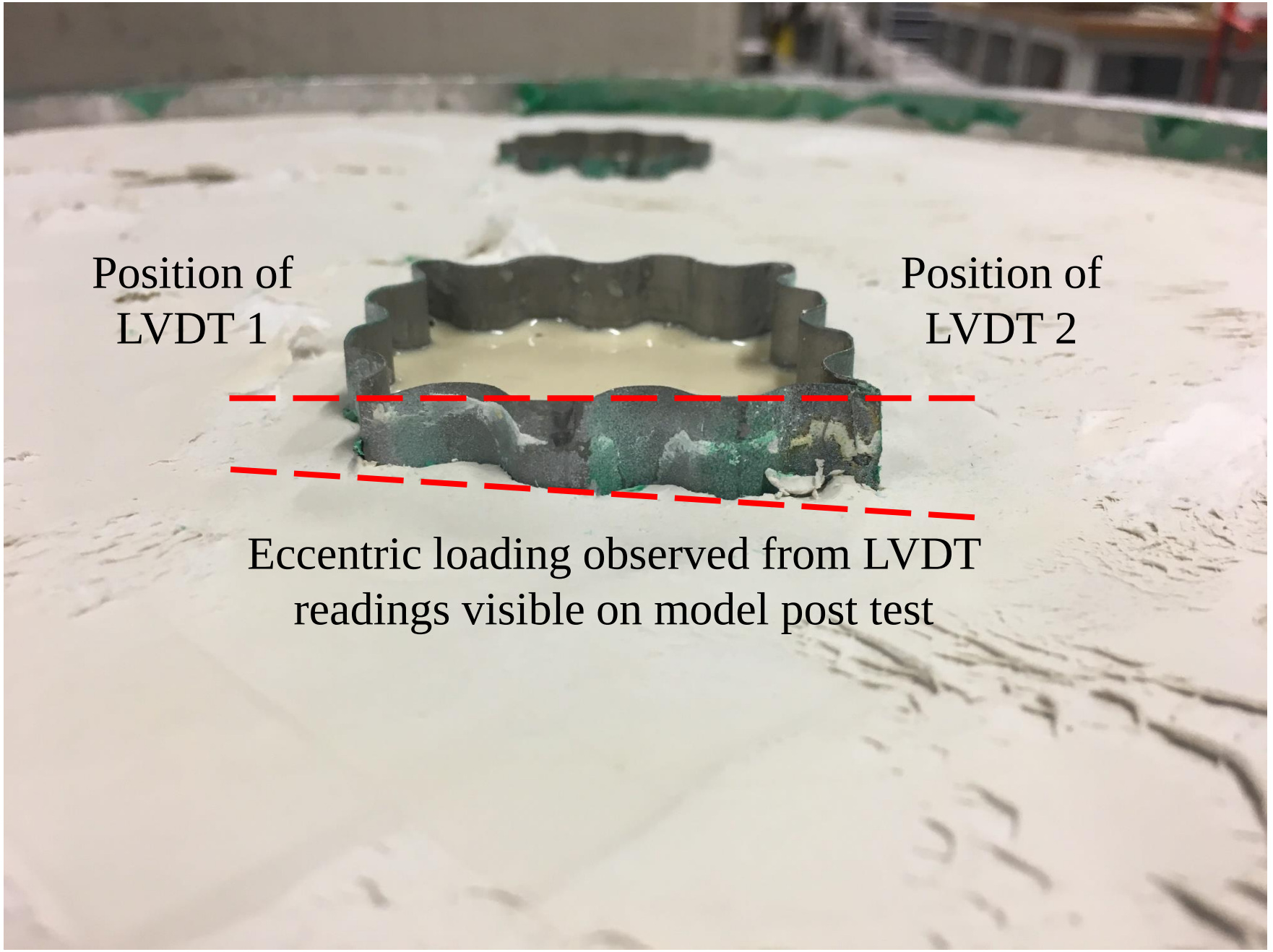
Position of
LVDT 1
Position of
LVDT 2
Eccentric loading observed from LVDT
readings visible on model post test

TABLES

TABLE 1: Nominal dimensions of piles

	Solid circular pile (smooth and rough)	Sheet piles		
		Circular sheet pile	Large square sheet pile	Small square sheet pile
Plan outline of pile	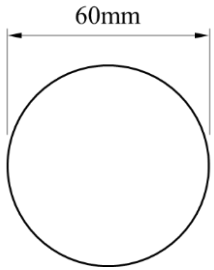	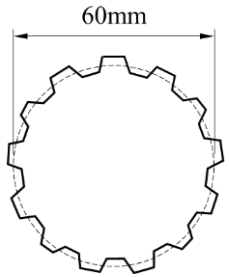	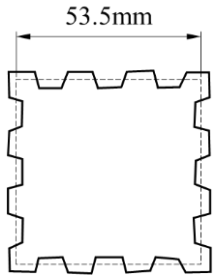	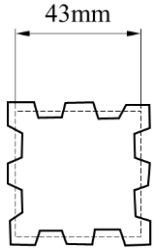
Nominal width/diameter (mm)	60	60	53.5	43
Measured perimeter (mm)	188	217	246	214
Computed base area (mm^2)	2827	2827	2862	1849

* Note: the embedded lengths of all piles in this series of tests were 180mm

TABLE 2; summary of centrifuge tests carried out

Test number	Model pile 1	Model pile 2	Comments
1	Solid circular – smooth (no sand)	Circular sheet pile (no perforations)	Solid pile became buoyant
2	Solid circular – rough (no sand)	Circular sheet pile (no perforations)	Buoyant pile
3	Solid circular – smooth	Circular sheet pile (perforated)	
4	Solid circular – rough	Circular sheet pile (perforated)	Unresponsive load cell on sheet pile
5	Solid circular pile – rough	Square sheet pile (large)	Unconsolidated sample
6	Square sheet pile (small)	Square sheet pile (large)	
7	Square sheet pile (large)	Circular sheet pile (perforated)	Unresponsive load cell on square sheet pile

TABLE 3; Measured loads and calculated α values from centrifuge tests

		Measured			Back calculation		
Test	**Model pile**	**Average $Su_{(vane)}$ along pile shaft (kN/m^2)**	**Load at 1% normalised settlement (kN)**	**Ultimate load* (kN)**	**α value at 1%**	**α value at ultimate state**	**Comments**
1	Solid circular – smooth (no sand)	45	0.46	0.82	**-0.825**	**-0.589**	Buoyant pile
1	Circular sheet pile	45	0.59	1.16	**-0.153**	**0.171**	
2	Solid circular – rough (no sand)	50	1.405	2.17	**-0.229**	**0.222**	Buoyant pile
2	Circular sheet pile	50	0.767	1.368	**-0.066**	**0.241**	
3	Solid circular – smooth	49.5	1.004	1.38	**-0.485**	**-0.261**	
3	Circular sheet pile (perforated)	49.5	0.96	1.694	**0.026**	**0.406**	
4	Solid circular – rough	48	1.405	2.074	**-0.132**	**0.279**	
4	Circular sheet pile (perforated)	48	-	-	**-**	**-**	Unresponsive load cell
5	Solid circular pile – rough	42	1.142	1.919	**-0.283**	**0.262**	Unconsolidated sample
5	Square sheet pile (large)	42	1.36	2.307	**0.305**	**0.815**	
6	Square sheet pile (small)	42	0.881	1.334	**0.236**	**0.516**	
6	Square sheet pile (large)	42	1.344	1.852	**0.310**	**0.584**	
7	Square sheet pile (large)	51	-	-	**-**	**-**	Unresponsive load cell
7	Circular sheet pile (perforated)	51	1.315	2.124	**0.160**	**0.566**	

*Note: ultimate load defined as 10% normalised settlement

TABLE 4: Summary of back calculated values of *α* at the ultimate state

Pile type	**Plan of pile**	**Test reference**						
		1	2	3	4	5	6	7
		Back calculated α values from $Su_{(vane)}$						
Rough solid circular pile		-	0.222	-	0.279	0.262	-	-
Circular sheet pile		0.171	0.241	-	-	-	-	-
Perforated circular sheet pile		-	-	0.406	-	-	-	0.566
Large square sheet pile		-	-	-	-	0.815	0.584	-
Small square sheet pile		-	-	-	-	-	0.516	-